JOURNAL OF MATERIALS SCIENCE 26 (1991) 5327–5334

Effects of TiO_2 addition on the sintering of $ZrO_2 \cdot TiO_2$ compositions and on the retention of the tetragonal phase of zirconia at room temperature

V. C. PANDOLFELLI, J. A. RODRIGUES
Universidade Federal de S. Carlos, DEMa, C.P. 676, CEP 13560, S. Carlos, SP, Brazil
R. STEVENS
School of Materials, University of Leeds, Leeds LS2 9JT, UK

The production of tetragonal zirconia polycrystalline (TZP) ceramics and the identification of factors controlling retention of the tetragonal phase in the $ZrO_2 \cdot TiO_2$ system have been investigated. In this binary system, it was not possible to retain tetragonal zirconia polycrystals at room temperature for a range of compositions sintered above 1200 °C. A decrease in the martensitic transformation temperature of zirconia with titania addition was observed, but the effect was insufficient to retain the tetragonal phase at room temperature. In solid solution, the TiO_2 additions act to suppress ZrO_2 densification, this leading to grain growth when attempts are made to attain higher densities. The use of fine powders, fast firing or sintering in reducing conditions altered densification but was not able to generate a final grain size sufficiently small to avoid spontaneous tetragonal→monoclinic transformation on cooling. Based on the results obtained for $ZrO_2 \cdot MO_x$ systems, the main factors involved in the retention of tetragonal zirconia at room temperature are discussed in an attempt to incorporate thermodynamical and the stress field effects.

1. Introduction

Zirconia engineering ceramics have received considerable attention in recent years. At the present time, by control of the microstructure and stabilizer content, tetragonal zirconia polycrystals (TZP) can be produced to give desired combinations of strength and toughness. Economics dictates the requirement for inexpensive stabilizer additives to zirconia in order to retain the tetragonal form for the development of optimum properties.

Although no definitive version of the $ZrO_2 \cdot TiO_2$ phase diagram is yet available [1], at first sight TiO_2 appears to be a good candidate additive, considering the large tetragonal zirconia solid solution range and the low eutectoid temperature developed in this system (Fig. 1).

In the present study, zirconia-based ceramics in the $ZrO_2 \cdot TiO_2$ system have been investigated with the following objectives:

(a) to attempt the production of tetragonal zirconia polycrystalline ceramic using compositions and conditions hitherto not investigated;

(b) to obtain further understanding of the factors that could lead to tetragonal zirconia retention at room temperature.

2. Experimental procedure

Powders were prepared by coprecipitation of zirconium *n*-propoxide and titanium isopropoxide in a continuously stirred H_2O/NH_4OH solution maintained at pH = 10. After separation from the liquid, the precipitate was washed three times with isopropyl alcohol. Following drying at 80 °C, the powders were calcined at 950 °C for 30 min and subsequently micronized in an alcohol suspension using cylindrical zirconia media. The calcination programme was based on the results of thermogravimetric and differential thermal analysis. A standard multi-point gas adsorption technique was used to evaluate the surface area of the powders prior to sintering and of the densified pellets after sintering.

X-ray fluorescence (XRF) spectrometry was used to analyse the composition of all calcined powders in the $ZrO_2 \cdot TiO_2$ system. To provide reproducible and accurate analyses, the fusion technique was utilized to prepare samples of both the standards and unknown compositions. Fusion helped to overcome problems arising from particle size, surface state and absorption effects.

The sintering behaviour of green compacts was investigated under isothermal conditions in air and also in reducing atmospheres using a sinter dilatometer. On the assumption that isotropic shrinkage was taking place during sintering, a computer program converted the LVDT voltage reading into specimen density. Using curve fitting routines, the densification rates which occurred at different times were

0022–2461/91 $03.00 + .12

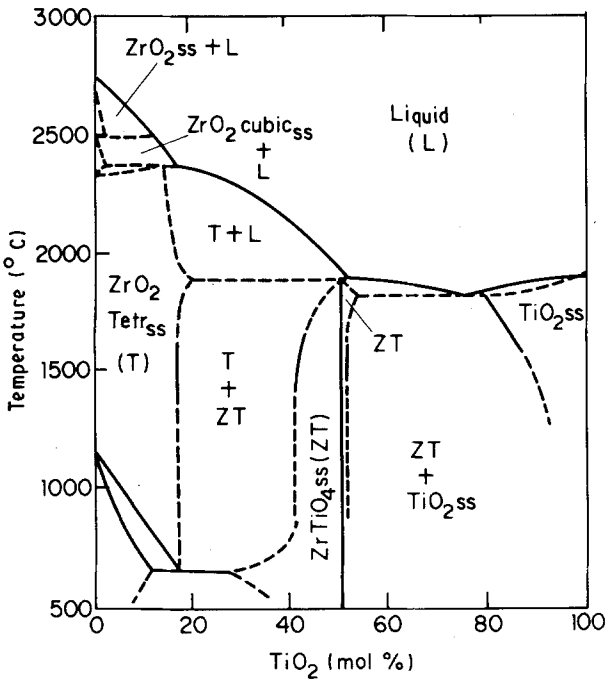

Figure 1 Tentative phase diagram of $ZrO_2 \cdot TiO_2$ system [1].

obtained. For the reducing conditions, a mixture of 8 vol p.m. carbon dioxide in 5.01 vol % carbon monoxide balanced with argon was used as the sintering atmosphere.

Phase analysis and lattice parameter determination of the calcined powders and sintered discs were performed using an X-ray diffractometer with Ni-filtered Cu radiation. The volume fraction of the monoclinic (m) and tetragonal (t) phases present were calculated using Toraya's equation [2] assuming the constant $P = 1.31$.

3. Results

A range of compositions in the $ZrO_2 \cdot TiO_2$ system was prepared by changing the amount of TiO_2 present. An average of 0.8 mol % Hf was detected in the zirconia produced by coprecipitation of the alkoxides. The similar chemical properties of ZrO_2 and HfO_2 allow the latter to be considered as equivalent to zirconia for compositional calculations.

Quantitative phase analyses, lattice volume and the ratio between the (0 0 4) and (4 0 0) lattice parameters for the $ZrO_2 \cdot TiO_2$ powders calcined at 950 °C are shown in Table I. Phases other than monoclinic or tetragonal solid solutions of zirconia were not found to be present in the calcined powders.

For the sintering experiments, the calcined powders were die-pressed at 190 MPa. Using heating and cooling rates of 300 °C h^{-1}, the pellets were sintered at 1350, 1450 and 1550 °C for 2 h. Results for the green and final sintered density are given in Table II.

After sintering, the tetragonal phase had not been retained in any of the range of compositions. With the exception of the composition without TiO_2 and that with 21.5 mol % TiO_2, all the samples sintered at 1550 °C were found to have fallen apart in the sintering furnace as a consequence of the martensitic $t \rightarrow m$ transformation during cooling. The presence of $ZrTiO_4$ has been confirmed only in the compositions with 17.9 and 21.5 mol % TiO_2. Results of a similar nature were obtained by Bateman [3] studying the $ZrO_2 \cdot 15$ mol % TiO_2 composition.

Using a sinter dilatometer with controlled atmosphere, the changes of density with time, and the densification rate with density were obtained. Fig. 2 shows the effect of TiO_2 addition on the densification rate of zirconia sintered in air at 1200 °C. Only the monoclinic zirconia phase was detected for all the

TABLE I Quantitative phase analysis, cell volume and tetragonal lattice parameter ratio (c/a) for the $ZrO_2 \cdot TiO_2$ powders calcined at 950 °C

Composition (mol %)	Tetragonal volume fraction (%)	Volume (nm^3)	c/a
92.4 ZrO_2–7.6 TiO_2	25.3 ± 0.2	0.13362	1.0236 ± 0.0005
88.5 ZrO_2–11.5 TiO_2	70.4 ± 1.6	0.13360	1.0250 ± 0.0003
85.2 ZrO_2–14.8 TiO_2	94.0 ± 0.6	0.13324	1.0265 ± 0.0001
82.1 ZrO_2–17.9 TiO_2	100	0.13305	1.0294 ± 0.0004
78.5 ZrO_2–21.5 TiO_2	100	0.13295	1.0317 ± 0.0001

TABLE II Green and final density of $ZrO_2 \cdot TiO_2$ compositions sintered at different temperatures

Composition (mol %)	Green density (%)	Final relative density (%)		
		1350 °C	1450 °C	1550 °C
ZrO_2	41.16 ± 1.71	89.53 ± 0.68	92.62 ± 0.86	91.25 ± 0.86[a]
92.4 ZrO_2–7.6 TiO_2	39.39 ± 1.13	90.67 ± 2.80[a]	82.46 ± 0.70[a]	c.d.[b]
88.5 ZrO_2–11.5 TiO_2	38.10 ± 1.06	74.49 ± 5.64[a]	c.d.	c.d.
85.2 ZrO_2–14.8 TiO_2	38.47 ± 0.71	73.91 ± 2.67[a]	85.48 ± 2.13[a]	c.d.
82.1 ZrO_2–17.9 TiO_2	38.41 ± 1.08	51.16 ± 0.18	73.96 ± 4.29[a]	c.d.
78.5 ZrO_2–21.5 TiO_2	38.17 ± 0.90	45.77 ± 0.90	60.04 ± 0.70	95.34; 1.08[a]

[a] Large amount of microcracks.
[b] c.d. = complete destruction.

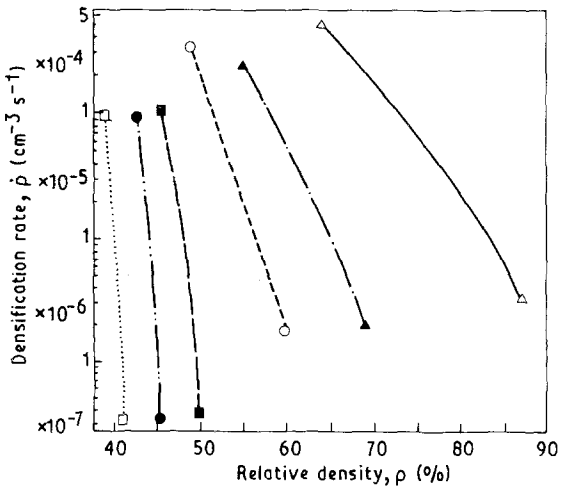

Figure 2 Densification rate versus relative density for $ZrO_2 \cdot TiO_2$ compositions sintered in air (A) at 1200 °C. Each curve represents the best fit for a range of 50 data points. Z = ZrO_2, T = TiO_2. (△) Z/0T(A), (▲) 92.37 Z/7.63 T(A), (○) 88.47 Z/11.53 T(A), (■) 85.21 Z/14.78 T(A), (●) 82.11 Z/17.89 T(A), (□) 78.47 Z/21.53 T(A).

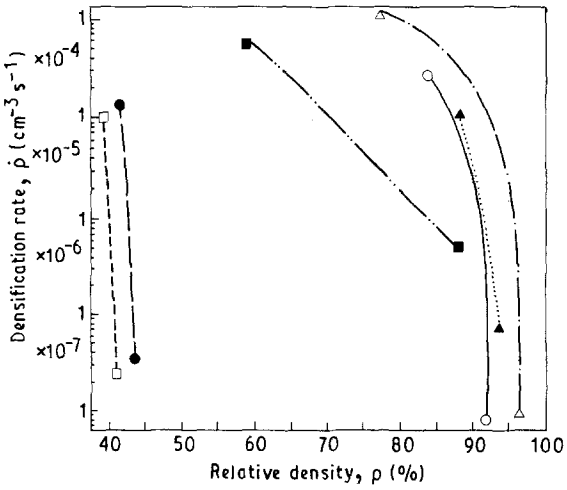

Figure 3 Densification rate versus relative density for ZrO_2 and 78.5 ZrO_2–21.5 TiO_2 mol % composition sintered in air (A) and reducing atmosphere (R), at (○, ▲, ■, △) 1450 °C, (□, ●) 1200 °C, (○) Z/0T(A), (▲) Z/0T(R), (□, ■) 78.47 Z/21.53 T(A), (●, △) 78.47 Z/21.53 T(R).

compositions when sintering took place at 1200° C. Results in Fig. 2 clearly indicate that when in solid solution, the increase in TiO_2 addition is inhibiting the densification of zirconia, resulting in a reduced final density.

The influence of air and reducing atmosphere on the sinterability of ZrO_2 and the 78.5 $ZrO_2 \cdot 21.5$ TiO_2 mol % composition is presented in Fig. 3. The oxygen partial pressure was calculated using Turkdogan tables [4] as being 2.4×10^{-19} atm at 1200 °C and 1.84×10^{-16} atm at 1450 °C. Tetragonal zirconia was not retained for any of the compositions sintered under reducing conditions.

To study the influence of TiO_2 on the transformation temperature of the zirconia alloys, measurements have been carried out to determine the temperature range for the martensitic transformation. Table III shows the start and finish of the t⇌m transformation during cooling (M_s and M_f temperature, respectively) and on heating (A_s and A_f). No further changes in the transformation temperature were observed when compositions in the $ZrO_2 \cdot TiO_2$ system were sintered in reducing atmospheres.

Because the driving force for both the densification and coarsening processes is related to the reduction in surface area, Burke *et al.* [5] suggested that materials with different coarsening and densification behaviour should be distinguished by the different shape of their surface area reduction trajectories. Considering a graph where surface area is plotted against relative density, for the case of pure coarsening, the surface area will be reduced with no increase in density, as shown by trajectory A in Fig. 4. When the reduction of the surface area is occurring wholly by mechanisms that result in densification, then trajectory B is obtained. The more typical sintering behaviour of real compacts is described by a series of curves between the two extremes, due to the simultaneous contributions of both mechanisms.

In order to obtain further information concerning the influence of TiO_2 on the sinterability of ZrO_2, the model of Burke *et al.* [5] was applied to the $ZrO_2 \cdot TiO_2$ system. The results for $ZrO_2 \cdot TiO_2$ compositions sintered for different times at 1200 °C are shown in Fig. 5 and represent an average of at least three measurements for each sample.

TABLE III Influence of TiO_2 on the martensitic transformation temperature of ZrO_2

Composition (mol %)	M_s (°C)	M_F (°C)	A_s (°C)	A_F (°C)
ZrO_2	925	830	1090	1160
92.4 ZrO_2–7.6 TiO_2	775	730	990	1060
88.5 ZrO_2–11.53 TiO_2	692	656	840	910
85.2 ZrO_2–14.8 TiO_2	559	537	750	820
82.1 ZrO_2–17.9 TiO_2	431	410	570	700
78.5 ZrO_2–21.5 TiO_2	326	220	454	640

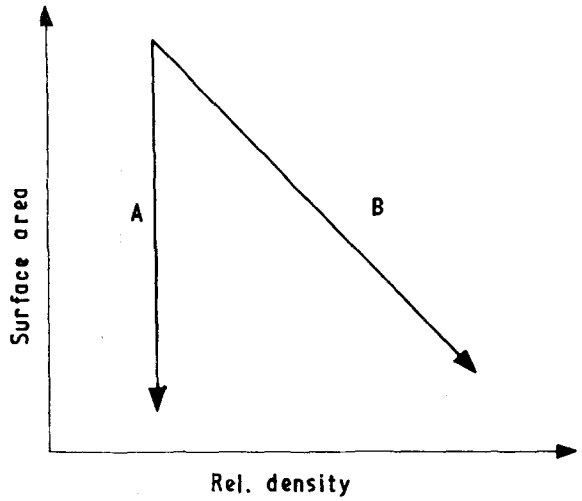

Figure 4 Surface area and relative density relationship during sintering. A is the trajectory for pure coarsening and B that for pure densification.

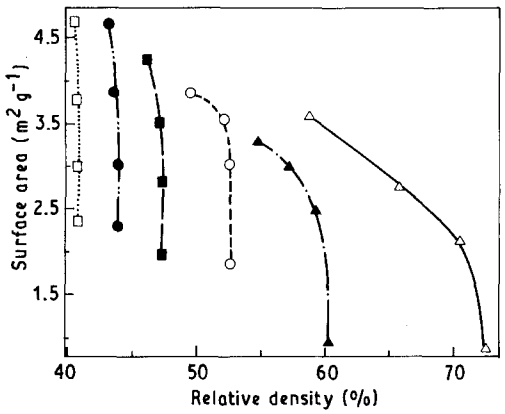

Figure 5 Surface area versus relative density for pellets of $ZrO_2 \cdot TiO_2$ compositions sintered for different times at 1200 °C. (△) Z/0T, (▲) 92.37 Z/7.63 T, (○) 88.47 Z/11.53 T, (■) 85.21 Z/14.78 T, (●) 82.11 Z/17.89 T, (□) 78.47 Z/21.53 T.

Improvements in densification with a reduction of grain growth can be obtained by fast firing [6]. The effectiveness of this process can be understood in terms of the difference of the activation enthalpies for the densification and coarsening mechanisms [7]. In materials where the enthalpies for lattice and boundary diffusion are higher than for surface diffusion, the higher the sintering temperature, the larger will be the densification/coarsening ratio. Data for activation enthalpies of the relevant diffusion species necessary to calculate the coefficients are not at present available and therefore the best way to assess the operating mechanisms is by experiment.

Fast firing experiments were therefore carried out in a tube furnace at temperatures of 1400, 1500 and 1600 °C. The pellets, laid on a highly porous alumina base, were automatically pushed into the hot zone of the furnace taking ~ 120 s to reach the maximum temperature. After a dwell time of 15 min they were moved to a region of the furnace at 200 °C. All the experiments were repeated using commercial tetragonal zirconia (TS–12 Ce and TS–3Y) and pure commercial zirconia (Dynazirkon (R)F) to establish whether thermal shock damage would affect interpretation of the results. Compositions containing titania resulted in complete disintegration after fast firing for 15 min at 1400, 1500 and 1600 °C. Table IV shows the effect of fast firing at 1600 °C on the resultant density.

To verify whether any remnant product of the calcination in the powders prepared by the alkoxide route could cause the differences in densification behaviour found amongst the $ZrO_2 \cdot TiO_2$ compositions, infrared spectrographic analysis was performed. The powders, 0, 14.8 and 21.5 mol % TiO_2, were calcined at 850, 1100 and 1300 °C. A heating rate of 300 °C h^{-1} and a dwell time of 1 h at the maximum temperature was used for all the calcinations. The samples for infrared analysis were prepared by careful mixing and vacuum pressing of 3 mg calcined powders with 300 mg KBr. The transmission infrared spectra of the calcined powders were determined over the range 4000–500 cm^{-1}.

TABLE IV Final density of zirconia pellets after fast firing at 1600 °C for 15 min

Composition	Final density ($g cm^{-3}$)
Dynazirkon (R) F	5.05 ± 0.01
TS–12CE (12 mol % CeO_2)	5.64 ± 0.02
TS–3Y (3 mol % Y_2O_3)	5.89 ± 0.01
ZrO_2	5.41 ± 0.07
All compositions in the $ZrO_2 \cdot TiO_2$ system	Disintegration

The results obtained show that all three powders calcined at 850 °C have bands which can be assigned to the C–H and O–H bond stretching. The presence of the bands can be associated with residues from the alkoxides reaction. After calcination at higher temperatures, oxidation of the residues is complete and the bands are no longer present. The presence of monoclinic zirconia is verified by bands at 740 and 515 cm^{-1} in the spectrum of zirconia calcined at 850 °C. The intensity of this band is greatly reduced in the powder with 14.8 mol % TiO_2 calcined at this temperature and is not apparent in the spectrum of the composition containing 21.5 mol % TiO_2. On calcination at higher temperatures the intensity of the monoclinic absorption band increases for all three compositions in agreement with the XRD results.

In a final experiment to ascertain the influence of the nature of the powder on the sinterability of zirconia–titania compositions, commercial zirconia, Dynazirkon (R)F, and commercial rutile, Tioxide, were wet ball milled in the same proportions as were present in the powders prepared by the alkoxide route. The mixed powders were then calcined at 950 °C and were found not to show any tetragonal stabilization. The presence of a strong rutile peak in the XRD trace inferred that the extent of take-up of TiO_2 into solid solution was limited. For the mixed oxide powders, the final densities of pellets sintered at 1200 and 1350 °C for 2 h did not show a large decrease in relative density as the TiO_2 is incorporated into the zirconia. However, XRD shows that complete solid solution has not taken place, suggesting that the TiO_2 agglomerates had sintered and that some of the TiO_2 had not been taken into solid solution. Tetragonal zirconia was not detected in any of the experiments involving mixtures of the commercial powders. Results obtained from the mixed powders experiments have demonstrated the necessity for using the alkoxide route to produce suitable powders in order to study the effect of TiO_2 on the sintering and stabilization of ZrO_2.

4. Discussion

In the $ZrO_2 \cdot TiO_2$ system, when sintering took place above 1200 °C, it was found that the t⇌m transformation had not been sufficiently suppressed to retain tetragonal zirconia at room temperature.

The reasons for retention of metastable tetragonal zirconia at room temperature are still the subject of considerable discussion. Provided the same grain

morphology exists and there is an absence of a glassy phase at the grain boundary, other factors that could be of importance in controlling retention of the tetragonal phase include:

(a) as thermodynamical considerations: the size, charge and concentration of dopant ions; the crystal structure of the dopant ion and the concentration and the role of anion vacancies;

(b) in relation to kinematical and stress field considerations: the thermal expansion anisotropy and the effect of the dopant ion on the sintered microstructure of the zirconia host.

The different factors that influence stabilization and hence retention of metastable and stable tetragonal zirconia may well be inter-related; however, discussion of how each variable might individually affect the $ZrO_2 \cdot TiO_2$ system will help to identify which is of greatest significance.

It is known that oxygen vacancies created either by reducing the oxygen partial pressure or by alloying zirconia with aliovalent metal oxides (Mg^{2+}, Ca^{2+} and Y^{3+}) play an important role in stabilizing the cubic structure [8–10]. Stabilization of the cubic phase can be considered as the thermodynamic response of the system to the need for accommodation of a large number of anion vacancies produced during sintering [11]. Although a decrease of the cubic–tetragonal transformation temperature for low p_{O_2} is shown in the Zr–O phase diagram [8], previous researchers have indicated that the tetragonal to monoclinic transformation remains unaffected by p_{O_2} [12, 13]. This opinion might well need modification because the presence of stabilizer additions such as CeO_2 can, at temperatures in excess of 1000 °C, lead to a reduction in the oxidation state of the cerium ion. This would be accompanied by a corresponding increase in the concentration of oxygen ion vacancies. However, the presence of oxygen vacancies can induce changes in the number of chemically bound nearest neighbours and can also affect the diffusion rate, particularly of oxygen ions.

It can be seen in Fig. 3 that defects generated by TiO_2, either (i) by increasing the temperature, or (ii) sintering in reducing conditions, are important in increasing the $ZrO_2 \cdot TiO_2$ sinterability. However, the presence of such defects did not manifest itself in any positive effect on the retention of tetragonal zirconia at room temperature.

In comparison with the ZrO_2–CeO_2 system, a fully tetragonal zirconia is obtained when a composition with 12 mol % ceria is sintered in air, provided that the final grain size remains below 3–4 μm. It is known that above 685 °C, CeO_2 may exhibit large deviations from stoichiometry, which may extend to a maximum at $CeO_{1.78}$ at and above 1023 °C [14]. Experiments undertaken as part of this study show that sintering ceria-stabilized tetragonal zirconia in a reducing atmosphere gives monoclinic zirconia plus $Ce_2Zr_2O_7$ [15]. Therefore, if the presence of oxygen vacancies is important for tetragonal stabilization in the $ZrO_2 \cdot CeO_2$ system, then perhaps the concentration of oxygen vacancies should be limited such that the CeO_{2-x} component remains in solid solution (Fig. 6), therefore avoiding formation of the second phase.

Thus although the influence of oxygen vacancies in cubic zirconia stabilization has been ascertained, in general their significance with respect to the retention of tetragonal zirconia at room temperature remains unclear in respect to the $ZrO_2 \cdot TiO_2$ and $ZrO_2 \cdot CeO_2$ systems.

The cationic radius and the crystal symmetry of the dopant are further important parameters contributing to zirconia stabilization and its retention. Titanium (Ti^{4+} = 0.074 nm) [17] has a smaller cationic radius than zirconium (Zr^{4+} = 0.084 nm) and tetragonal zirconia polycrystalline ceramics (TZP) have not been produced using this ion. On the other hand, cations such as magnesium (Mg^{2+} = 0.089 nm), cerium (Ce^{4+} = 0.097 nm), yttrium (Y^{3+} = 0.1019 nm) and calcium (Ca^{2+} = 0.112 nm), in which the ionic radius is larger than that of Zr^{4+}, have all been used to stabilize zirconia ceramics. With respect to the crystal structure of the dopants mentioned above, it appears that only solute oxides having a cubic structure are able to stabilize the cubic and/or to retain the tetragonal phase in zirconia. MgO and CaO both have a cubic NaCl structure, CeO_2 has a cubic fluorite structure, Y_2O_3 a cubic bixbyite structure, whereas TiO_2 has a tetragonal rutile structure [18]. Although results related to the cationic radius and crystal symmetry of the most common dopants (MgO, CaO, Y_2O_3 and CeO_2) could indicate that those ions having a larger diameter than zirconia and forming oxides with a cubic structure would be more likely to produce TZP ceramics, this trend cannot be generalized. Dopants such as Nd_2O_3, Yb_2O_3, Gd_2O_3, Eu_2O_3 and La_2O_3 all have the same crystal structure as Y_2O_3 and a cationic radius larger than zirconia, but so far fully tetragonal zirconia polycrystals have not yet been produced using these oxides [19, 20].

A consistent factor pertaining to tetragonal zirconia retention is the critical grain size for spontaneous

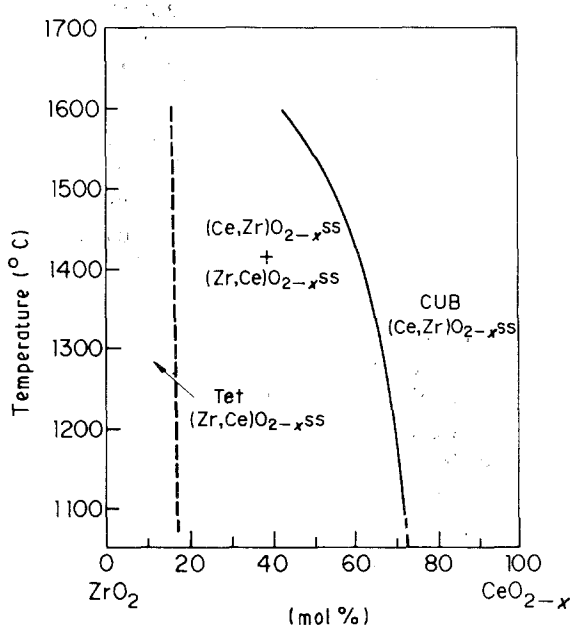

Figure 6 The system $ZrO_2 \cdot CeO_{2-x}$ in air, in the 1100–1600 °C temperature range [16].

$t \rightleftharpoons m$ transformation. Heuer and Rühle [21] and Chen and Chiao [22] in their analyses, suggested the critical grain size at a given temperature can be defined as the size below which the probability of each grain containing a critical nucleus is less than unity. Typically it is less than 3 μm for the CeO_2–TZP and is in the range 0.5–1.0 μm for Y_2O_3–TZP.

Table III and the phase diagram of the $ZrO_2 \cdot TiO_2$ system (Fig. 1) show that TiO_2 additions reduce the chemical free energy for the $t \rightleftharpoons m$ phase transformation but give no indication of how TiO_2 might affect the final grain size of zirconia. Applying Burke's model to the $ZrO_2 \cdot TiO_2$ system (Fig. 5), this shows that on addition of titania, the densification component is gradually reduced until almost pure coarsening occurs for the 78.5 ZrO_2–21.5 TiO_2 mol % composition. These results were confirmed by grain size measurements on the polished surfaces of the 21.5 mol % TiO_2 composition ceramics.

For systems which do not densify significantly, vapour transport and surface diffusion have been suggested as the predominant mass transport mechanisms. Vapour transport occurs by an evaporation–condensation process and the extent to which it occurs depends on the vapour pressure of the material being sintered. For most oxides in use as engineering ceramics, vapour phase transport is usually only of importance at very high temperatures, close to the melting point. In the $ZrO_2 \cdot TiO_2$ system, owing to the low volatility of zirconium and titanium oxide [23], it is to be expected that surface diffusion would play a major role in the coarsening process at low temperature. Titania might act to inhibit sintering in zirconia by increasing the surface diffusion coefficient in the material and hence increasing the coarsening rate. Other researchers agree that TiO_2 additions accelerate grain growth and act to suppress densification in Y_2O_3–TZP ceramics [24, 25]. Osendi and Moya [26] showed that although TiO_2 increases the initial sintering rate of the Al_2O_3–8 vol % ZrO_2 composites, a significant enhancement of the grain growth kinetics of ZrO_2 was observed after annealing.

In order to avoid coarsening and promote sintering, three principal procedures can be utilized.

(a) Fine, homogeneous powder. In the present study, the use of a fine, chemically homogeneous powder produced by the alkoxide route was found not to give a dense ceramic after sintering. The decrease of sinterability with TiO_2 additions to ZrO_2 cannot, therefore, be associated with the powder preparation route, because surface area results, agglomerate strength, electron microscopy and infrared analysis showed no significant property or morphological differences between the powders.

(b) Fast firing. Fast firing was ineffective in generating the small grain size required to retain the tetragonal phase. Measurements of final density after fast firing a range of $ZrO_2 \cdot TiO_2$ compositions was not possible; however, the final grain size was obviously above the critical size because the martensitic transformation could not be avoided.

(c) Hot pressing. Hot-pressing experiments undertaken using graphite punches and a graphite die led to a partial reduction of the zirconium oxide and also to the formation of titanium carbide. The use of an alumina punch and die set was considered, but was found not to be feasible due to the chemical reactions which could occur between the sample and the alumina die.

In consequence, the principal techniques used to produce enhanced density are all problematical in that difficulties are encountered in the retention of the desirable fine grain size or modifications to the resulting microstructure are produced.

5. Conclusions

1. In the $ZrO_2 \cdot TiO_2$ system, it has not been possible to retain tetragonal zirconia polycrystals at room temperature for compositions sintered above 1200 °C. Despite the decrease in temperature (the martensitic transformation) of zirconia with titania additions, this in itself was insufficient to retain the tetragonal phase at room temperature.

2. The lattice defects generated by sintering $ZrO_2 \cdot TiO_2$ compositions in a reducing atmosphere have improved densification but did not show any positive effect on the retention of the tetragonal zirconia at room temperature. Studies carried out in the $ZrO_2 \cdot TiO_2$ system, the $ZrO_2 \cdot CeO_2$ system, and an analysis of results available in the literature, show that the influence of oxygen vacancies, cationic radius and crystal structure of dopant on stabilization of tetragonal zirconia is yet to be clearly explained.

3. In solid solution, TiO_2 additions to ZrO_2 act to suppress the densification, leading to grain growth when attempts are made to attain higher densities. This is believed to be the main factor preventing retention of tetragonal zirconia at room temperature in the $ZrO_2 \cdot TiO_2$ system. The use of fine powders and fast firing techniques was not able to keep the final grain size small enough to avoid spontaneous $t \rightleftharpoons m$ transformation on cooling.

Acknowledgements

V. C. Pandolfelli thanks CNPq process no. 20.2522/84 for sponsoring his studies at Leeds University. The helpful discussions with Professor R. J. Brook and Dr I. Nettleship were also greatly appreciated.

Appendix. Zirconia sintering in reducing conditions

For zirconia pellets with the same initial green density, Fig. 3 shows that sintering in reducing atmosphere yielded a slightly higher densification rate than pellets sintered in air. Assuming that (i) sintering at low p_{O_2} increases the concentration of oxygen vacancies, and (ii) the rate-controlling species for densification in zirconia is cationic [10], because the diffusion coefficients of cations in zirconia are several orders of magnitude less than the values for oxygen (Table AI), the results of Fig. 3 can only be explained if the concentra-

TABLE AI Diffusion coefficients of oxygen and zirconium in pure zirconia [27]

Temperature (°C)	Log D ($cm^2\ s^{-1}$)	
	Oxygen	Zirconium
1100	− 12	− 17
1300	− 6	− 14
1900	−	− 11

tion of cationic defects increases at a greater rate than the oxygen vacancy concentration.

In order to explain this possibility further, the defect chemistry of zirconia has been examined and analysed.

At low p_{O_2}, the concentration of oxygen vacancies $[V_O^{\cdot\cdot}]$ is assumed to be greater than the concentration of zirconium vacancies ($V_{Zr}^{''''}$], oxygen interstitials $[O_i'']$, electron holes (p)* and zirconium interstitials $[Zr_i^{\cdot\cdot\cdot\cdot}]$. Thus the following electroneutrality conditions can be set

$$2[V_O^{\cdot\cdot}] = n \quad \text{(A1)}$$

Applying the mass-action relationship for the defect equilibria equations below

$$O_O^x = V_O^{\cdot\cdot} + 2e' + \tfrac{1}{2}O_{2(g)} \quad \text{for low } p_{O_2} \quad \text{(A2)}$$

$$\text{zero} = V_{Zr}^{''''} + 2V_O^{\cdot\cdot} \quad \text{(A3)}$$

$$\text{zero} = e' + h^{\cdot} \quad \text{(A4)}$$

$$O_O^x = V_O^{\cdot\cdot} + O_i'' \quad \text{(A5)}$$

$$Zr_{Zr}^x = V_{Zr}^{''''} + Zr_i^{\cdot\cdot\cdot\cdot} \quad \text{(A6)}$$

and using the neutrality condition (Equation A1), the following trends for the concentration of defects with the oxygen partial pressure are obtained

$$[V_O^{\cdot\cdot}] \propto [O_2]^{-1/6} \quad \text{(A7)}$$

$$[Zr_i^{\cdot\cdot\cdot\cdot}] \propto [O_2]^{-1/3} \quad \text{(A8)}$$

$$[O_i''] \propto [O_2]^{1/6} \quad \text{(A9)}$$

$$[V_{Zr}^{''''}] \propto [O_2]^{1/3} \quad \text{(A10)}$$

$$n \propto [O_2]^{-1/6} \quad \text{(A11)}$$

$$p \propto [O_2]^{1/6} \quad \text{(A12)}$$

It can be seen from Equations A7 and A8 that both $[V_O^{\cdot\cdot}]$ and $[Zr_i^{\cdot\cdot\cdot\cdot}]$ increase at significantly different rates as the oxygen partial pressure is reduced in the range where the neutrality condition is valid (Fig. A1).

Under such conditions, the increased rate of $[Zr_i^{\cdot\cdot\cdot\cdot}]$ formation compared with $[V_O^{\cdot\cdot}]$, i.e. $[O_2]^{-1/3}$ as compared with $[O_2]^{-1/6}$ respectively, could explain the higher densification rate shown by the zirconia pellets sintered in a reducing atmosphere. The present results agree with those obtained by Wu [28] when sintering zirconia in air, with different amounts of CaO added.

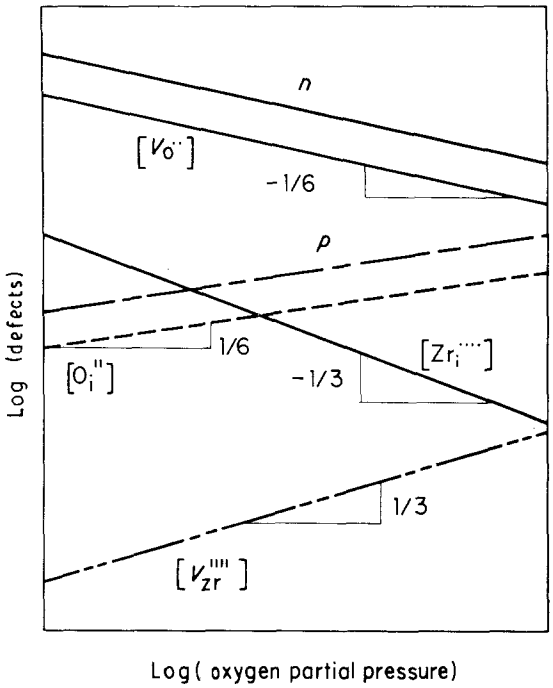

Figure A1 Brouwer diagram, showing the variation of defect concentrations with oxygen partial pressure in pure zirconia. The neutrality condition assumed is $n = 2[V_O^{\cdot\cdot}]$.

References

1. T. NOGUCHI and M. MIZUNO, *Bull. Chem. Soc. Jpn* **41** (1968) 2695.
2. H. TORAYA, M. YOSHIMURA and S. SOMIYA, *J. Amer. Ceram. Soc.* **67** (1984) C119.
3. C. A. BATEMAN, MSc Dissertation, Lehigh University, USA (1986).
4. E. T. TURKDOGAN, in "Physical Chemistry of High Temperature Technology" (Academic Press, New York, 1980).
5. J. E. BURKE *et al., Mater. Sci. Res.* **13** (1979) 417.
6. S. WU, PhD thesis, Leeds University, UK (1982).
7. H. MOSTAGHACI and R. J. BROOK, *Trans. J. Br. Ceram. Soc.* **82** (1983) 167.
8. R. RUH and H. J. GARRET, *J. Amer. Ceram. Soc.* **50** (1967) 257.
9. A. H. HEUER and M. RÜHLE, in "Advances in Ceramics", Vol. 12, "Science and Technology of Zirconia 2", edited by N. Claussen, M. Rühle and A. H. Heuer (The American Ceramic Society, Columbus, Ohio, USA, 1983) p. 1.
10. S. M. HO, *Mater. Sci. Engng* **54** (1982) 23.
11. P. RAMASWAMY and D. C. AGRAWAL, *J. Mater. Sci.* **22** (1987) 1243.
12. S. C. CARNIGLIA, S. D. BROWN and T. F. SCHROEDER, *J. Amer. Ceram. Soc.* **54** (1971) 13.
13. E. G. RAUH and S. P. GARG, *ibid.* **63** (1980) 239.
14. P. KOFSTAD, in "Nonstoichiometry, Diffusion and Electrical Conductivity in Binary Metal Oxides" (Wiley Interscience, USA, 1972).
15. V. C. PANDOLFELLI, unpublished results, Leeds University, UK (1988).
16. S. R. ROTH, J. R. DENNIS and H. F. McMURDIE, in "Phase Diagrams for Ceramists", Vol. 6 (The American Ceramic Society, Westerville, Ohio, USA, 1987).
17. R. D. SHANNON, *Acta Crystallogr.* **A32** (1976) 751.
18. R. W. G. WYCKOFF, in "Crystal Structure", Vols 1 and 2 (Interscience, UK, 1964).
19. E. K. KÖHLER and V. B. GLUSHKOVA, in "Science of Ceramics 4", edited by G. H. Stewart (British Ceramic Society, UK, 1968) p. 233.
20. B. BASTIDE, P. ODIER and J. P. COVTURES, *J. Amer. Ceram. Soc.* **71** (1988) 449.
21. A. H. HEUER and M. RÜHLE, *Acta Metall.* **33** (1985) 2101.

* In the case of electrons and positive holes the concentration of these defects are often written as n and p, instead of [e'] and [h$^{\cdot}$] respectively.

22. I. W. CHEN and Y. H. CHIAO, in "Advances in Ceramics", Vol. 12. "Science and Technology of Zirconia 2", edited by N. Claussen, M. Rühle and A. H. Heuer (The American Ceramic Society, Columbus, Ohio, USA, 1983) p. 33.
23. M. S. CHANDRASEKHARAIAH, in "The Characterization of High Temperature Vapours", edited by J. L. Morgrave (Wiley Interscience, USA, 1976) p. 495.
24. J. TSUKUMA, *J. Mater. Sci. Lett.* **5** (1986) 1143.
25. T. SATO *et al.*, *Int. J. High Tech. Ceram.* **2** (1986) 167.
26. M. I. OSENDI and J. S. MOYA, *J. Mater. Sci. Lett.* **7** (1988) 15.
27. P. ALDEBERT and J. P. TRAVERSE, *J. Amer. Ceram. Soc.* **68** (1985) 34.
28. S. WU and R. J. BROOK, *J. Br. Ceram. Soc.* **82** (1983) 200.

Received 7 December 1990
and accepted 15 January 1991